Intracardiac Electrogram Transformation

Morphometric Implications for Implantable Devices

Milton M. Morris, MSE, Janice M. Jenkins, PhD, and Lorenzo A. DiCarlo, MD

Over 75,000 antitachycardia devices (ATDs) have been implanted since initial Food and Drug Administration approval in 1985 and have yielded dramatic survival rates. These devices, although life-saving, rely principally on simple measures of the heart rate for arrhythmia detection. The ATDs are highly sensitive, but their low specificity of diagnosis results in episodes of inappropriate therapy ranging as high as 10 to 41% of all shocks delivered (1–5).

Morphologically based algorithms have been demonstrated to improve levels of specificity dramatically while maintaining high levels of sensitivity (6–11); however, these algorithms tend to be computationally complex, placing unacceptably large demands on battery power (12,13). Since ATDs are small battery-operated implants, small algorithmic demands on battery power are essential for device longevity.

Correlation waveform analysis (CWA), a morphologically based algorithm, has emerged as a promising technique for more specific assessment of intracardiac electrogram (IEGM) rhythms. Correlation waveform analysis

From the Department of Electrical Engineering and Computer Science, University of Michigan and Michigan Heart and Vascular Institute, Ann Arbor, Michigan.

Reprint requests: Milton M. Morris, University of Michigan, 4421 EECS Building, Ann Arbor, MI 48109-2122.

has previously been demonstrated to separate monomorphic ventricular tachycardia (MVT) and ventricular fibrillation (VF) from sinus rhythm (SR) and performs as well, if not better, than other morphologically based algorithms when classifying MVT from SR (12). However, the power demand of CWA has led to its exclusion from ATD algorithm implementation. If the number of data points required for accurate analysis by CWA were sufficiently reduced, the diminished power demand concomitant with such a reduction could make CWA an attractive discriminant.

The Karhunen–Loeve transformation and feature selection of the IEGM was examined in this study to determine whether the Karhunen–Loeve transformation with feature selection yields increased specificity and reduced the power demand of morphologically based algorithms such as CWA. The Karhunen–Loeve transformation domain has useful and informative statistical properties, which make signal analysis simpler. In the Karhunen–Loeve transformation domain, data points (features) can be systematically selected that contain information required for accurate rhythm classification. This method of extracting data, feature selection, results in fewer data points for processing. Results of the Karhunen–Loeve transformation with feature selection may confirm CWA to be a feasible algorithm for consideration in ATD algorithm design.

A)

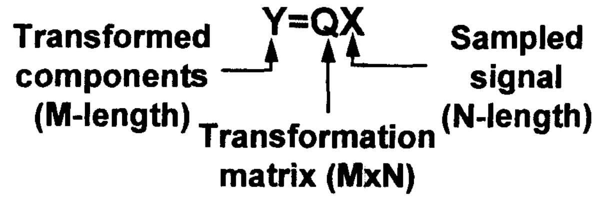

B)

$$X = \begin{bmatrix} x_1 \\ x_2 \\ x_3 \\ \vdots \\ x_N \end{bmatrix} \quad Y = \begin{bmatrix} y_1 \\ y_2 \\ y_3 \\ \vdots \\ y_N \end{bmatrix}$$

C)

$$K_Y = QK_XQ^T = \mathrm{Diag}(\lambda)$$

$$K_X = \mathrm{Cov}(X_1, X_2, X_3, .., X_N)$$

D)

$$X = y_1q_1 + y_2q_2 + ... + y_Nq_N = \sum_{i=1}^{N} y_iq_i$$

Fig. 1. (A) Linear transformation Y of the vector X through the transform matrix Q. (B) Vector X comprised of discrete samples of an observation. Vector Y generated via Q from vector X. (C) Covariance matrices for Y and X. (D) Expansion of X using eigenvectors as bases and y components as weighting.

Background

A digitized signal of length N can be analyzed as a point in N-dimensional space. The sample values of this digitized signal (the components of an N-length vector) describe the location of this point in N-dimensional space. A more efficient representation of the digitized signal X can be obtained by transforming X into an alternative space. Figure 1A shows such a transformation. Our new signal representation Y has been generated by a transformation of the original signal X (Fig. 1B) via the orthogonal transformation matrix Q (Fig. 1C). The vector Y is comprised of uncorrelated components, whereby each component exclusively contains information about the original signal X. For example, the jth component in vector Y contains information that cannot be obtained by any other component(s). Furthermore, components in vector Y contain various amounts of information about the original signal X and can be ordered accordingly using a normalized variance distribution (Fig. 2). From the normalized variance distribution, informed decisions may be made regarding which components contain the information required for adequate signal reconstruction or accurate signal classification/detection. For reconstruction purposes, theory suggests using the components associated with the largest variance. This is because the normalized variance expresses the percentage of error introduced by omitting the corresponding component during reconstruction of the original signal vector X (14). However, for purposes of classifying/detecting IEGMs and treating the normal SR signal as known exactly (through a template creation process), theory suggests using the data associated with small variances (15). In the classification/detection problem, the normalized variance may be interpreted as the amount of noise a particular component contains (ie, high variance means low signal-to-noise ratio). By choosing components associated with

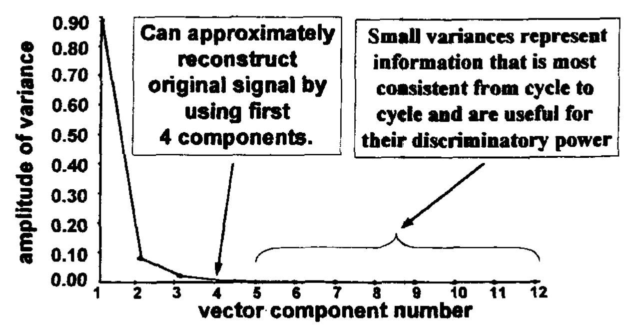

Fig. 2. Normalized variance distribution can represent a relative amount of information contained in Y component about original signal X (reconstruction problem) or the relative amount of noise in Y component (detection problem).

small variances, we remove large amounts of noise from data to be analyzed (ie, analyzed data have high signal-to-noise ratios). Once these components have been delineated, they may be systematically extracted from signals to be analyzed in the future. Both theoretical approaches result in a signal representation that is reduced in length and sufficient for the particular application (reconstruction or classification/detection).

The transformation matrix Q shown in Figure 1A is the Karhunen–Loeve transformation and is the optimum linear transformation in a mean squares sense. That is, the Karhunen–Loeve transformation minimizes the mean value of the squared error introduced when the original signal vector X is reconstructed using only a portion of the components comprising the transformed vector Y. The transformation is generated using second central moment statistics about the stochastic process X (ie, covariance matrix of X). Figure 1C shows the mathematical relationship between the Karhunen–Loeve transformation matrix and the covariance matrix of the signal X. Note that the covariance matrix of Y is created by pre- and postmultiplying the covariance matrix of X by the transformation matrix Q. Further note that the covariance matrix of Y is diagonal. Not only does this ensure that the Y components are uncorrelated but, more importantly, that the Karhunen–Loeve transformation is simply a matrix formed from the eigenvectors of the covariance matrix for X, and that the variances of each component of Y (the transformed signal vector) are simply the eigenvalues associated with these eigenvectors. Therefore, to generate the Karhunen–Loeve transformation for a particular patient record would (assuming no probability density function is known for the observation vector X) merely require a sufficient number of observation vectors X, subsequent generation of the sample covariance matrix for X, and a routine to generate the eigenvalues and eigenvectors of the covariance matrix.

The ease of data selection and the routine generation of the transformation itself makes the Karhunen–Loeve transformation an attractive feature in pattern recognition. Finally, the Karhunen–Loeve transformation is a rotation of the signal space such that each sample in the observation vector is fully uncorrelated, containing exclusive information about the original signal.

Materials and Methods

Intraventricular electrograms analyzed in this study were recorded from the right ventricular apex (1–500 Hz) during clinical cardiac electrophysiology studies of patients undergoing clinical evaluation and treatment. Written informed consent was obtained from each patient. Three 6F quadripolar electrode catheters (USCI Division, C.R. Bard, Billerica, MA) with an interelectrode distance of 1 cm were introduced and advanced under fluoroscopic guidance. Each electrode catheter had three platinum ring electrodes that were cylinders 2 mm in diameter and 2 mm in length. The platinum tip electrode of each catheter consisted of a half-sphere 2-mm diameter attached to a cylinder 2 mm in diameter and 1 mm in length. The resulting surface area of each ring and tip electrode was 12.6 mm^2. One electrode catheter was positioned in the high right atrium or right atrial appendage. Two electrode catheters were positioned in the right ventricular apex for right ventricular apex pacing and recording. Episodes of induced MVT and VF having a duration of 9 seconds or longer were recorded from a distal bipolar pair of the sensing catheter located in the right ventricular apex. Intracardiac electrograms were recorded continuously on FM magnetic tape at a tape speed of 3.75 inches (9.5 cm)/s (bandwidth of 0–1,250 Hz) (model 3968A, Hewlett-Packard, San Diego, CA) after signal amplification and filtering at 1–500 Hz. Amplifier gain and filter settings (V1205, Electronics-for-Medicine, PPG, Leneca, KS) were held constant during the entire recording procedure, and all electrogram amplitudes were computed using a 1-mV calibration signal entered as a reference at the time of recording. Each recording was assigned a case number and catalogued for subsequent off-line retrieval (Ann Arbor Electrogram Libraries, Ann Arbor, MI). Ten patients with diagnosed and documented episodes of normal SR, MVT, and VF were analyzed. The electrograms were filtered at 10–50 Hz. Data were digitized with a commercial A/D acquisition system (DATAQ, Akron, OH) at 120 Hz in accordance with the Nyquist criterion.

Analog data were filtered using a digitally tuned variable Krohn–Hite filter (series 3320, model 3323, Krohn–Hite Corporation, Avon, MA). The pass-band gain was unity (0 dB), with attenuation rates of 24 dB per octave outside the pass-band. Response characteristics were that of a four-pole, maximally flat Butterworth. The attenuation slope is nominally 24 dB per octave per channel in a low-pass or high-pass mode.

Computer Processing

Two variables affecting arrhythmia detection by ATDs analyzed in this study were signal transformation via the Karhunen–Loeve transformation and feature selection via variance thresholding. The classifier used for comparative analysis was the morphologic metric CWA. Individual complexes (depolarizations) were recognized using an auto-adjusting software trigger. A template of a normal ventricular electrogram was obtained for each patient by signal averaging 12 ventricular depolarization waveforms from episodes of normal SR to produce a representative waveform. Three pattern recognition systems were analyzed (Fig. 3): (1) normal, (2) Karhunen–Loeve transformation, and (3) Karhunen–Loeve transformation with feature selection. The Karhunen–Loeve transformation matrix was created for each patient from the same 12 ventricular depolarizations used to generate the representative waveform (template). Separate episodes of normal SR, VT, and VF were then processed by CWA on a cycle-by-cycle basis using the patient-specific normal SR template as a reference. The ventricular depolarization was

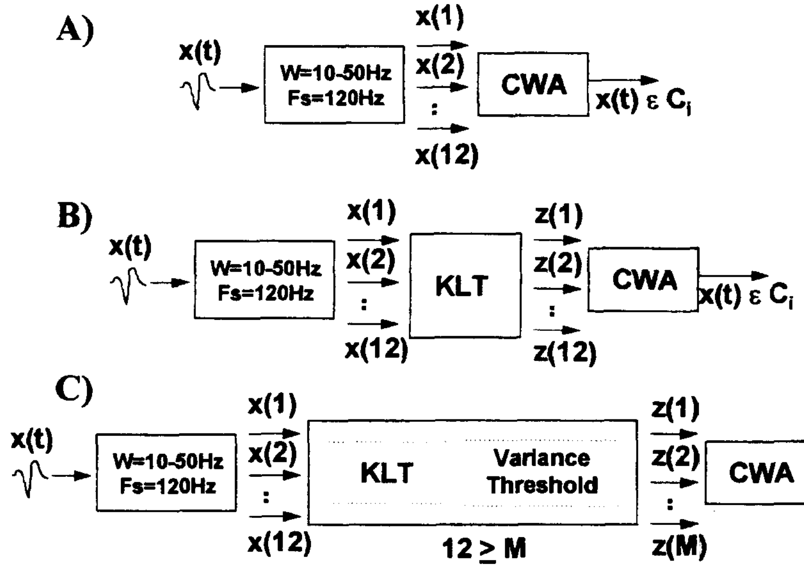

Fig. 3. (A) Pattern-recognition system 1 (PRS_1) sends normal data to be classified by correlation waveform analysis (CWA). (B) Pattern-recognition system 2 (PRS_2) sends transformed data to be classified by CWA. (C) Pattern-recognition system 3 (PRS_3) sends selected data to be classified by CWA. KLT, Karhunen–Loeve transformation.

found using a window starting at the trigger location and ending 12 data samples later. This corresponds to 100 ms of data per cycle. Twelve cycles were analyzed per episode and 36 cycles were analyzed per patient.

Statistics Applied for Analysis

Key statistics were generated using the cycle-by-cycle correlation coefficients of each episode. Each statistic was used individually as a method for classification. These statistics were the product of a pilot study we conducted that analyzed correlation coefficients in conjunction with the rhythms that produced them. It was determined that statistics measuring consistency (or inconsistency) would best classify normal SR, VT, and VF. The statistical metrics are described below.

1. Delta-CC = |max(CC) − min(CC)|. Because CC represents the normalized correlation coefficient yielding a value between +1 and −1, delta-CC yields a number between 0 and 2.
2. Standard deviation of the correlation coefficients.
3. Area = Delta-CC • Standard Deviation. Since area was derived by multiplying two statistics, the resultant value exaggerated the consistency (or inconsistency) and produced greater separation of distinct rhythms.
4. Volume = Area • $(\min|CC|)^{-1}$. Contains all of the qualities of the area statistic with more separation space (ie, larger statistical margin).

Results

The average specificity between the four key statistics used for classification purposes was calculated for all three pattern-recognition systems. Table 1 contains results further broken down into two tests: SR versus VT/VF and VT versus VF. Specificities were calculated with sensitivities held at 1, focusing attention on the effects that IEGM transformation (via the Karhunen–Loeve transformation) and feature selection have on specificity. Referring to Table 1, the average specificity for SR versus VT/VF is unchanged (0.988) when the Karhunen–Loeve transformation is used (PRS_2). The average specificity rises to 1.00 when both the Karhunen–Loeve transformation and feature selection are used (PRS_3). The average specificity for VT versus VF rises from 0.925 to 0.950 when the Karhunen–Loeve transformation is used (PRS_2), but decreases from 0.950 to 0.825 when the feature selection is used (PRS_3).

Table 2 provides information about the change in average correlation coefficient value for each rhythm and pattern-recognition system. The only significant change is the average correlation coefficient value for SR. The average correlation coefficient value for SR increases in all 10 patients when using just the Karhunen–Loeve transformation (PRS_2) and again (in all patients) when feature selection is added (PRS_3). The average correlation coefficients for VT and VF across all patients showed no significant change.

Table 3 gives insight into the effect of the Karhunen–Loeve transformation and feature selection on the statis-

Table 1. Average Specificity of Normal, Transformed and Selected Data for SR versus Disease and VT versus VF

	Average Specificity		
Test	Normal	Transformed	Selected
SR vs VT/VF	0.988	0.988	1.000
VT vs VF	0.925	0.950	0.825

SR, sinus rhythm; VF, ventricular fibrillation; VT, ventricular tachycardia.

Table 2. Increases in Average Value of Correlation Coefficients (out of 10 Episodes) for Each Rhythm Across All Pattern-recognition Systems

	Sinus Rhythm	Ventricular Tachycardia	Ventricular Fibrillation
Normal vs KLT	5/10	4/10	5/10
KLT vs selected	10/10	5/10	5/10
Normal vs selected	10/10	5/10	6/10

KLT, Karhunen–Loeve transformation.

tical marginal of separation. The statistical margin of separation is the difference between the statistics generated by each of the three rhythms. If the statistical margin of separation is increased, the algorithm is considered more powerful (assuming that the standard deviation of the statistics does not increase sufficiently to offset the change). In particular, Table 3 reveals how many times the statistical margin of separation used to classify rhythms increases (out of 40). The Karhunen–Loeve transformation alone (1st row) shows no significant effect on the statistical marginal of separation. Feature selection (2nd and 3rd rows) shows a propensity to decrease the statistical marginal of separation for SR versus VT and SR versus VF but no significant effect on VT versus VF.

Discussion and Conclusion

Because of the signal preconditioning, the correlation coefficients observed in this investigation where not typical of those found in general practice. The filter setting and sampling rate used in this study produced lower correlation coefficients with larger standard deviations across rhythms. The filter setting of 10–50 Hz has a differentiating effect that tends to add turning points to the IEGM signal (ie, a monophasic signal may become biphasic). Because of alignment difficulties, additional turning points effectively reduce the correlation coefficients (measures of likeness) of compared signals. The sampling rate of 120 Hz used in this investigation also strains the alignment accuracy and similarly effects the correlation coefficients. However, neither the filter setting nor the sampling rate adversely affect classification. The filter setting and sampling rate were found to be satisfactory in rhythm classification of the IEGM signal by CWA and were used to help reduce the number of data points to be processed by the computationally intense CWA (13).

Table 1 shows the performance by CWA using the four statistics for signal classification. The drastic increase in average specificity by PRS_3 (selected data) in the SR versus VT/VF test can be traced to decreased standard deviation of SR correlation coefficients and an increase in correlation coefficient values for SR when feature selection is implemented. The correlation coefficient values for VT and VF change but not in any uniform way. There is no significant change in the correlation coefficient values of SR using the Karhunen–Loeve transformation (PRS_2) versus not using it (PRS_1). This fact is corroborated (but not confirmed) by the maintenance of the level of specificity from PRS_1 to PRS_2. Table 2 shows the number of times the average correlation coefficient value increased when using the Karhunen–Loeve transformation alone (PRS_2) and when using it along with feature selection (PRS_3). There was no consistent effect on the average correlation coefficient value when using the Karhunen–Loeve transformation alone versus not using it and feature selection (PRS_1). The average correlation coefficient value increased in all 10 patients when using the Karhunen–Loeve transformation (PRS_3) relative to using the Karhunen–Loeve transformation alone (PRS_2)

Table 3. Statistical Marginal Increases in X of 40 (X/40) Statistics Across All Rhythms and Pattern-recognition Systems

	SR vs VT	VT vs VF	SR vs VF
Normal vs KLT	22/40	22/40	25/40
KLT vs selected	5/40	17/40	1/40
Normal vs selected	7/40	20/40	0/40

KLT, Karhunen–Loeve transformation; SR, sinus rhythm; VF, ventricular fibrillation; VT, ventricular tachycardia.

Table 4. Correlation Coefficient Means ± SDs for Each Rhythm and Pattern-recognition System

	Normal	Karhunen–Loeve Transformation	Selected
Sinus rhythm	0.904 ± 0.052	0.906 ± 0.050	0.989 ± 0.010
Ventricular tachycardia	0.310 ± 0.649	0.297 ± 0.653	0.405 ± 0.534
Ventricular fibrillation	0.126 ± 0.295	0.131 ± 0.310	0.160 ± 0.329

and not using it (PRS_1). The disease rhythms (VT and VF) were not similarly affected. In fact, the average correlation coefficients of VT and VF rhythms were not significantly affected by the additions of the Karhunen–Loeve transformation and feature selection (Table 4).

The Karhunen–Loeve transformation and feature selection can provide accurate rhythm classification and increased specificity when used with the morphometric CWA. By incorporating the Karhunen–Loeve transformation, we significantly affect only SR correlation coefficients, leaving MVT and VF correlation coefficients statistically unchanged. This discriminatory alteration of correlation coefficients allows for better classification of rhythms when using a selection criterion to extract certain features. Feature selection allows for systematic extraction and analysis of the aspects found most consistently in the IEGM of normal SR. Feature selection shows promise and warrants further study.

References

1. Echt DS, Armstrong K, Schmidt P et al: Clinical experience, complications and survival in 70 patients with automatic implantable cardioverter/defibrillator. Circulation 71:289, 1985
2. Steinberg JS, Sugalski JS, Haratonic K et al: Cardiac rhythm precipitating automatic implantable defibrillator discharges in outpatients: observations from transtelephonic recordings. (abstract) Circulation 80: 530, 1989
3. Gabry MD, Brodman R, Johnston D et al: Automatic implantable cardioverter-defibrillator: patient longevity and shock delivery analysis. J Am Coll Cardiol 9:1349, 1987
4. Grimm W, Flores BF, Marchlinski FE: Electrocardiographically documented unnecessary, spontaneous shocks in 241 patients with implantable cardioverter defibrillators. PACE 15(part I):1667, 1992
5. Sandler MJ, Kutalek SP: Inappropriate discharge by an implantable cardioverter defibrillator: recognition of myopotential sensing using telemetered intracardiac electrograms. PACE 17(part I):665, 1994
6. Stephany G, Ropella K: Real-time estimation of a magnitude-square coherence for use in implantable devices. p. 375. In Computers in cardiology. IEEE Computer Society, New York, 1992
7. Langberg JL, Gibbs WJ, Auslander DM et al: Identification of ventricular tachycardia with use of the morphology of the endocardial electrogram. Circulation 77:1363, 1988
8. Jenkins JM, DiCarlo LA, Chiang CM: Impact of filtering upon ventricular tachycardia identification by correlation waveform analysis. PACE 14(11-II):1 809, 1991
9. Throne RD, Jenkins JM, DiCarlo LA: The bin area method: a computationally efficient technique for analysis of ventricular and atrial intracardiac electrograms. PACE 13:1286, 1990
10. Finelli CJ, Li P, Jenkins JM et al: Intraventricular electrogram morphology: effect of increased heart rate with and without accompanying changes in sympathetic tone. p. 115. In Computers in cardiology. IEEE Computer Society, New York, 1990
11. Santel D, Mehra R, Olson W et al: Integrative algorithm for detection of ventricular tachyarrhythmias from the intracardiac electrogram. p. 175. In Computers in cardiology. IEEE Computer Society, New York, 1990
12. Jenkins JM, Caswell SA: Signal processing and detection algorithms in implantable cardiac devices. IEEE Proceedings 84:428, 1996
13. Morris MM, Jenkins JM, DiCarlo LA: Bandlimited morphometric analysis of the intracardiac signal implications for antitachycardia devices. PACE (in press)
14. Fukunaga K: Introduction to statistical pattern recognition. Academic Press, New York, 1972
15. Van Trees HL: Detection, estimation and modulation theory. John Wiley, New York, 1968